SLAC-PUB-8742
BABAR-PROC-00/31
hep-ex/0101035
January, 2001

Physics at *BABAR*

Christos Touramanis
University of Liverpool
Department of Physics, Oliver Lodge Laboratory
L69 7ZE , Liverpool , U.K.
(for the *BABAR* Collaboration)

Abstract

The *BABAR* detector at the SLAC PEP-II asymmetric e^+e^- collider has first started collecting data in May 1999. A study of time-dependent *CP*-violating asymmetries in $B^0 \to J/\psi K^0_S$ and $B^0 \to \psi(2S)K^0_S$ decays has been performed on a data sample of $9.0\,\mathrm{fb}^{-1}$ taken at the $\Upsilon(4S)$ resonance and $0.8\,\mathrm{fb}^{-1}$ off-resonance, collected through July 2000. The preliminary result $\sin 2\beta = 0.12 \pm 0.37\,(\mathrm{stat}) \pm 0.09\,(\mathrm{syst})$ is presented here, together with preliminary results on neutral and charged B meson lifetimes and $B^0\overline{B}^0$ mixing.

5th International Symposium on Radiative Corrections
(RADCOR–2000)
Carmel CA, USA, 11–15 September, 2000

Stanford Linear Accelerator Center, Stanford University, Stanford, CA 94309

Work supported in part by the U.K. Particle Physics and Astronomy Research Council, Advanced Research Fellowship GR/L04177 and Department of Energy contract DE-AC03-76SF00515.

1 Introduction

The three–generation Standard Model can accommodate *CP* violation through the presence of a non-zero imaginary phase in the Cabibbo-Kobayashi-Maskawa (CKM) quark mixing matrix. However, existing measurements of *CP* violation in the neutral kaon system cannot prove that the CKM phase is indeed the origin of *CP* violation in nature.

The primary goal of the *BABAR* experiment at PEP-II is to elucidate this question by a series of observations and measurements of *CP*–violating effects in the B meson system. These measurements allow the extraction of the angles α, β and γ of the Unitarity Triangle, whose non–zero area [1] is a direct measure of *CP* violation.

BABAR can also access the sides of the Unitarity Triangle through measurements of $|V_{ub}|$, $|V_{cb}|$ in semileptonic B decays and $|V_{td}|$ in $B^0\overline{B}^0$ mixing. This allows to overconstrain the Unitarity Triangle and perform stringent tests of the Standard Model.

Thus, high statistics, a clean environment and broad access to the rich phenomenology of the B sector will allow *BABAR* to improve our knowledge of the overall B decay picture and probe New Physics at higher energy scales. A broad heavy flavor physics programme is also ongoing in *BABAR*.

2 PEP-II

The PEP-II B Factory [2] is an e^+e^- colliding beam storage ring complex at SLAC designed to produce a luminosity of 3x10^{33} cm^{-2}s^{-1} at a center–of–mass energy of 10.58 GeV ($\Upsilon(4S)$ resonance). During the 2000 run PEP-II has exceeded this luminosity, while *BABAR*, with a logging efficiency of >95%, has routinely accumulated data above its design daily rate of 135 pb^{-1}.

The machine has asymmetric energy beams, with a High Energy Ring (HER, 9.0 GeV electrons) and a Low Energy Ring (LER, 3.1 GeV positrons). These correspond to a center–of–mass boost of $\beta\gamma$=0.56 and lead to an average separation of $\beta\gamma c\tau$=250 μm between the two B mesons vertices, allowing the measurement of time–dependent *CP*–violating decay rate asymmetries.

At the $\Upsilon(4S)$ resonance B mesons can only be produced as B^+B^- or coherent $B^0\overline{B}^0$ pairs. The time evolution of a coherent $B^0\overline{B}^0$ pair is coupled in such a way that the *CP* or flavor of one B at decay time t_1 can be described as a function of the other B (B_{tag}) flavor at its decay time t_2 and the signed time difference $\Delta t = t_1 - t_2$.

3 *BABAR*

3.1 Detector description [2]

The volume within the 1.5T *BABAR* superconducting solenoid contains a five layer silicon strip vertex detector (SVT), a central drift chamber (DCH), a quartz-bar Cherenkov radiation detector (DIRC) and a CsI(Tl) crystal electromagnetic calorimeter (EMC). Two layers of cylindrical resistive plate counters (RPCs) are located between the barrel calorimeter and the magnet cryostat. The instrumented flux return (IFR) outside the cryostat is composed of 18 layers of radially increasing thickness steel, instrumented with 19 layers of planar RPCs in the barrel and 18 in the endcaps which provide muon and neutral hadron identification.

3.2 Particle reconstruction and identification [2]

Charged particle tracking using the SVT and DCH achieves a resolution of $(\delta p_T/p_T)^2 = (0.0015\,p_T)^2 + (0.005)^2$, where p_T is the transverse momentum in GeV/c. The SVT with a typical resolution of $10\,\mu$m per hit provides excellent vertex resolution both in the transverse plane and in z. The typical fully reconstructed single B decay vertex resolution in z is $50\,\mu$m. Photons are reconstructed in the EMC, yielding mass resolutions of 6.9 MeV/c^2 for $\pi^0 \to \gamma\gamma$ and 10 MeV/c^2 for $K_S^0 \to \pi^0\,\pi^0$.

Leptons and hadrons are identified using a combination of measurements from all the *BABAR* components, including the energy loss $\mathrm{d}E/\mathrm{d}x$ in the helium-based gas of the DCH (40 samples maximum) and in the silicon of the SVT (5 samples maximum). Electron identification is mainly based on the characteristics of their shower in the EMC, while muons are identified in the IFR and confirmed by their minimum ionising signal in the EMC. Excellent kaon identification in the barrel region is provided by the DIRC, which achieves a separation of $>3.4\sigma$ in the range 0.25–3.5 GeV/c.

4 B reconstruction

A variety of inclusive, semiexclusive and exclusive reconstruction methods are applied on the *BABAR* data, covering semileptonic and pure hadronic decay modes. The corresponding B samples have different sizes and purity levels and are used for different types of studies (Branching Fraction measurements, studies of the dynamics of certain decay chains). We will focus here on the cases where some information (final state(s), charge, *CP* or flavor content, decay vertex) can be reconstructed for both B mesons in the event.

4.1 Exclusive B sample

B^0 and $B^\pm$ mesons are reconstructed in the following hadronic modes of definite flavor: $B^0 \to D^{(*)-}\pi^+, D^{(*)-}\rho^+, D^{(*)-}a_1^+$, $J/\psi\ K^{*0}$, $B^- \to D^0\ \pi^-$ and $B^- \to D^{*0}\ \pi^-$ [1]. All final state particles are reconstructed. The selections have been optimised for signal significance, using on–peak, off–peak and simulated data. Charged particle identification, mass(or mass difference) and vertex constraints are used wherever applicable. The signal for each decay mode is identified in the two-dimensional distribution of the kinematical variables ΔE and m_{ES}: $\Delta E = E^*_{\mathrm{rec}} - E^*_b$ is the difference between the B candidate energy and the beam energy and $m_{\mathrm{ES}} = \sqrt{E^{*2}_b - \boldsymbol{p}^{*2}_{\mathrm{rec}}}$ is the mass of a particle with a reconstructed momentum $\boldsymbol{p}^*_{\mathrm{rec}} = \sum_i \boldsymbol{p}^*_i$ assumed to have the beam energy, as is the case for a true B meson. In events with several B candidates only the one with the smallest ΔE is considered. The ΔE and m_{ES} variables have minimal correlation. The resolution in m_{ES} is $\approx$3 MeV/c^2 and is dominated by the beam energy spread. The resolution in ΔE is mode dependent and varies in the range of 12–40 MeV. For each mode a rectangular signal region is defined by the three standard deviation bands in m_{ES} ($5.27 < m_{\mathrm{ES}} < 5.29$ GeV/c^2) and ΔE (mode dependent interval). For each mode the sample composition is determined by fitting the m_{ES} distribution for candidates within the signal region in ΔE to the sum of a single Gaussian representing the signal and a background function introduced by the ARGUS collaboration [3]. The purity of each subsample is computed as the ratio of the area of the Gaussian in the $\pm 3\sigma$ range over the total area in this range. Figure 1 shows the m_{ES} distributions for the summed hadronic B^0 and $B^\pm$ modes with the fits superimposed.

[1] Throught this paper, conjugate modes are implied.

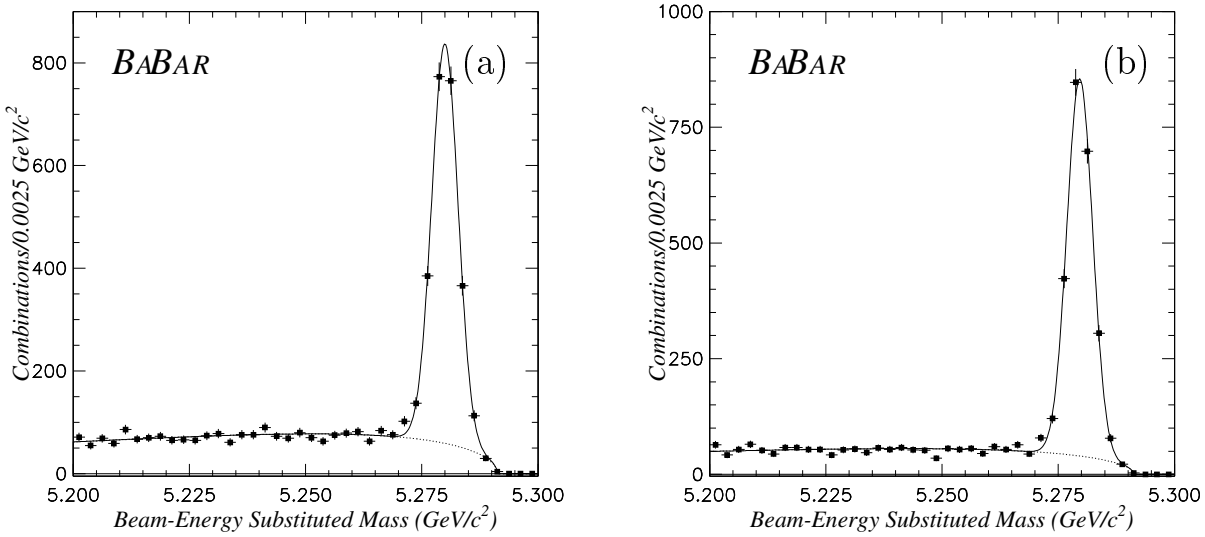

Figure 1: $m_{\rm ES}$ distribution for all the hadronic modes for (a) B^0 and (b) $B^{\pm}$. The complete fit and its ARGUS [3] background content are also shown. The number of signal events in all B^0 and $B^{\pm}$ modes are 2577 ± 59 and 2636 ± 56, with purity of ≈86% and ≈89% respectively.

4.2 Flavor tagging

After removal of the daughter tracks of the reconstructed B_{rec} in an event, the remaining tracks are used to determine the flavor of the other B meson (B_{tag}), and this ensemble is assigned a tag flavor, either B^0 or $\overline{B}^0$.

For each of the tagging methods used we define an effective tagging efficiency $Q_i = \varepsilon_i \times (1-2w_i)^2$, where ε_i is the fraction of events tagged by this method i and w_i is the mistag fraction, *i.e.* the probability of incorrectly assigning the opposite tag to an event using this method. A dilution factor is defined as $\mathcal{D} = 1 - 2w$ and is extracted from the data for each method.

The `Lepton` category uses the presence and charge of a primary lepton from the decaying b quark. Both electrons and muons are used, with a minimum center-of-mass momentum requirement of 1.1 GeV/c. If both an electron and a muon candidate satisfy this requirement, only the electron is taken into account. Mistag arises from (a) pions seen as leptons and (b) softer opposite-sign leptons coming from charm semileptonic decays.

The `Kaon` category is based on the total charge of all identified Kaons. Events with conflicting `Lepton` and `Kaon` tags are excluded from both categories.

For events not tagged with the previous methods, a variety of available particle identification and kinematic variables are fed in a Neural Network whose design and training aims at exploiting the information present in this set of correlated quantities. It is sensitive to the presence of primary and cascade leptons, charged kaons and soft pions from D^* decays. In addition, the charge of high-momentum particles is exploited in a "jet-charge" type approach. This functionality has been assigned to different sub–nets, to facilitate understanding of the network performance. The output from the full neural network tagger x_{NT} is mapped onto the interval $[-1, 1]$. The assigned flavor

tag is B^0 if x_{NT} is negative, and $\overline{B}^0$ otherwise. Events with $|x_{NT}| > 0.5$ are assigned to the `NT1` tagging category and events with $0.2 < |x_{NT}| < 0.5$ to the `NT2` tagging category. Events with $|x_{NT}| < 0.2$ have very little tagging power and are rejected.

4.3 Δt calculation and resolution

Since no stable charged particle emerges from the $\Upsilon(4S)$ decay point, the production point of the B mesons and thus their individual decay times cannot be determined. However the decay time difference Δt between the two is sufficient for the description of a coherent B meson pair (decay length difference technique).

The event topology is sketched in Fig. 2. In the *boost approximation* used in *BABAR* the decay time difference is calculated as : $\Delta t = \Delta z / c < \beta\gamma >$, where the small flight path of the B mesons perpendicular to the z exis is ignored.

Actually, the small effects arising from the tilt of the PEP-II beams with respect to the *BABAR* z axis (20 mr), fluctuations in the beam energies, the B meson transverse momentum in the $\Upsilon(4S)$ rest frame, have been studied and are taken into account either in the calculations or in the systematic errors as appropriate.

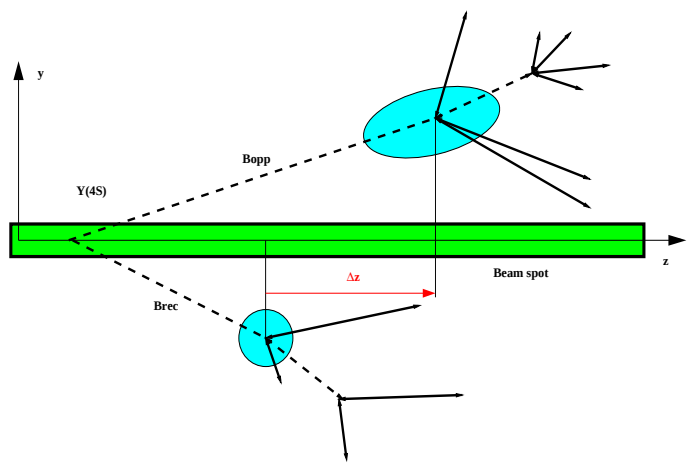

Figure 2: Event topology showing the two B production and decay points. The figure is not drawn to scale; it has been expanded in the y direction.

The resolution σ_z for the fully reconstructed B is found in the simulation to be 45–65 μm, depending on the mode. The resolution σ_z for the tag side is $\approx$125 μm, with a small bias of 25 μm due to forward–going charm decays that cannot be resolved. The resulting resolution in Δt has been parametrised as the sum of three gaussians. The core has a σ of 0.6 ps and contains 75% of the events. The tail has a σ of 1.8 ps. Outliers are described by a gaussian with fixed σ of 8 ps, that contains $\approx$1% of the total events. This resolution model is used for the lifetime, mixing and sin2β fits. Two scale factors (multiplicative to the width of the core and tail gaussians) are included in the fits to the real data for the first two cases, to account for eventual imperfections in the modeling of D decays and multiple scattering in the simulation. Extensive studies on the different event samples and with variations of the fits (free and fixed parameters) have been performed in order to optimise and validate the method and to obtain reliable estimates of the systematic errors.

5 B lifetime measurements

The observed Δt distribution for a set of B pair events in the presence of the resolution function $\mathcal{R}$ is :

$$\mathcal{F}(\Delta t) = \Gamma \exp(-\Gamma|\Delta t|) \otimes \mathcal{R}(\,\Delta t\,;\,\hat{a}\,) \tag{1}$$

where $\hat{a}$ is the set of parameters describing the resolution function.

The B meson lifetimes are extracted with unbinned maximum likelihood fits that take individual event Δt errors into account. Our preliminary results are :

$$\begin{aligned} \tau_{B^0} &= 1.506 \pm 0.052 \text{ (stat)} \pm 0.029 \text{ (syst) ps} \\ \tau_{B^+} &= 1.602 \pm 0.049 \text{ (stat)} \pm 0.035 \text{ (syst) ps} \\ \tau_{B^+}/\tau_{B^0} &= 1.065 \pm 0.044 \text{ (stat)} \pm 0.021 \text{ (syst)} \end{aligned}$$

The only background source is combinatorial and it is estimated from the side-bands of the beam energy substituted mass variable. The main systematic error comes from the resolution modeling and parameters. The two proper time fits are shown in Figure 3.

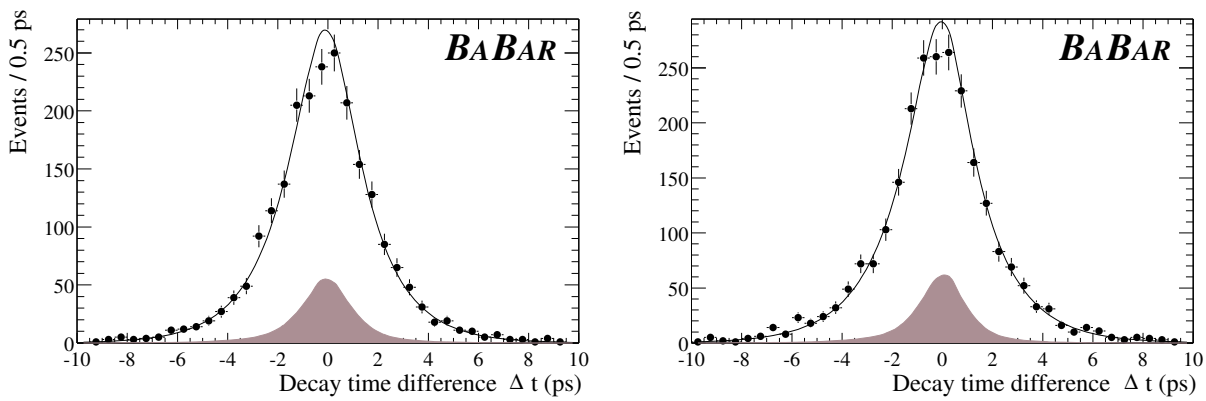

Figure 3: Δt distributions for the B^0 (right) and $B^\pm$ (left) candidates. The result of the lifetime fit is superimposed. The hatched areas represent the background content of the event samples.

6 B^0 mixing measurements

Mixing allows the two neutral B mesons in the $B^0\overline{B}^0$ coherent state to decay with the same flavor (*mixed events*) or the opposite flavor (*unmixed events*). In a perfect detector one would then observe a time dependent oscillation in the rates of unmixed(+) and mixed(-) events :

$$f_\pm(\Delta t;\,\Gamma,\,\Delta m_d) = \frac{1}{4}\,\Gamma\,\mathrm{e}^{-\Gamma|\Delta t|}\,[\,1 \pm \cos\Delta m_d\,\Delta t\,] \tag{2}$$

where Δm_d is the difference between the mass eigenstates B^0_H and B^0_L. Due to imperfect tagging and vertex determination the observed rates become :

$$\mathcal{F}_\pm(\Delta t;\,\Gamma,\,\Delta m_d,\,\mathcal{D},\hat{a}\,) = \frac{1}{4}\,\Gamma\,\mathrm{e}^{-\Gamma|\Delta t|}\,[\,1 \pm \mathcal{D} \times \cos\Delta m_d\,\Delta t\,] \otimes \mathcal{R}(\,\Delta t\,;\,\hat{a}\,) \tag{3}$$

where $\mathcal{D}$ is the dilution factor (section 4.2) and $\mathcal{R}$ is the Δt resolution (section 4.3)

An unbinned maximum likelihood fit that takes into account individual event Δt errors and tagging category is performed on events from the exclusively reconstructed B^0 sample (section 4.1), after tagging (section 4.2) has been performed. The value of Δm_d is fitted simultaneously with the individual dilution factors for each tagging category. This information is later used in the sin2β extraction. Our preliminary result for Δm_d is :

$$\Delta m_d = 0.516 \pm 0.031(\text{stat.}) \pm 0.018(\text{syst.})\hbar\,\text{ps}^{-1}$$

A sample of events where a semileptonic ($D^*\ell\nu$) instead of a hadronic B^0 decay has been reconstructed (7517 events) are analysed using the same method and fit. The preliminary result for Δm_d from this sample is :

$$\Delta m_d = 0.508 \pm 0.020(\text{stat.}) \pm 0.022(\text{syst.})\hbar\,\text{ps}^{-1}$$

Combining the Δm_d results from the hadronic and semileptonic B samples we obtain the preliminary result :

$$\Delta m_d = 0.512 \pm 0.017(\text{stat.}) \pm 0.022(\text{syst.})\hbar\,\text{ps}^{-1}$$

The main sources of systematic errors are the Δt resolution function, Monte Carlo statistics and the $B^\pm$ background in the semileptonic sample.

In an independent analysis a more abundant but less pure sample of dilepton events has been used. In this inclusive approach the mistag arising from cascade leptons and the $B^\pm$ fraction are extracted from the same fit as Δm_d. Our preliminary result for Δm_d is :

$$\Delta m_d = 0.507 \pm 0.015(\text{stat.}) \pm 0.022(\text{syst.})\hbar\,\text{ps}^{-1}$$

The results from the hadronic and dilepton samples are shown in Figure 4. The tagging performance parameters for each tagging method (category) are extracted from the fully reconstructed sample fits (hadronic and semileptonic) and are shown in Table 1.

Tagging Category	ε (%)	w (%)	Q (%)
`Lepton`	11.2 ± 0.5	$9.6 \pm 1.7 \pm 1.3$	7.3 ± 0.7
`Kaon`	36.7 ± 0.9	$19.7 \pm 1.3 \pm 1.1$	13.5 ± 1.2
`NT1`	11.7 ± 0.5	$16.7 \pm 2.2 \pm 2.0$	5.2 ± 0.7
`NT2`	16.6 ± 0.6	$33.1 \pm 2.1 \pm 2.1$	1.9 ± 0.5
all	76.7 ± 0.5		27.9 ± 1.6

Table 1: Tagging preformance parameters measured from the mixing maximum-likelihood fit for the fully-reconstructed B^0 sample. The uncertainties on ε and Q are statistical only.

7 The sin2β measurement

If one of the neutral B mesons(B_{tag}) of the coherent $B^0\overline{B}^0$ pair decays to a definite flavor eigenstate at time t_{tag} and the other B decays to a CP–even eigenstate like $J/\psi K^0_S$ or $\psi(2S)K^0_S$ at time t_{CP},

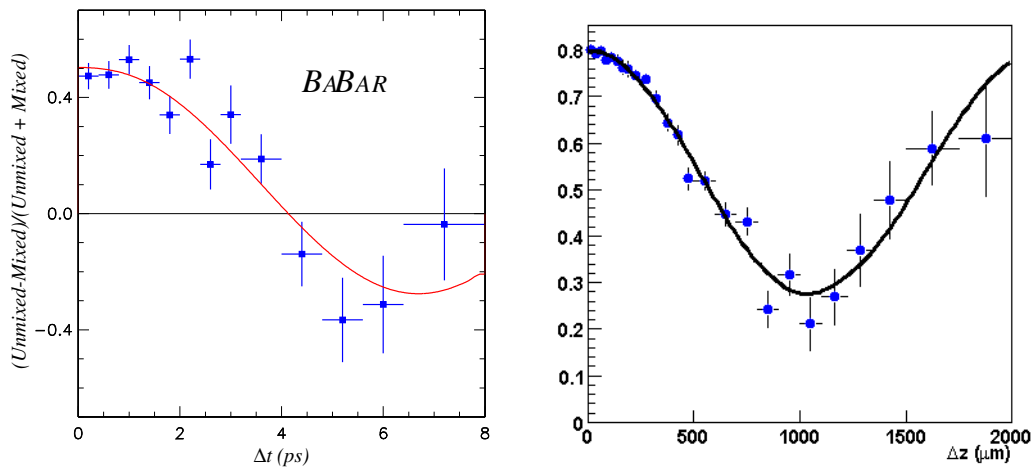

Figure 4: The observed time dependent asymmetries between unmixed and mixed events for the fully reconstructed (left) and dilepton (right) B^0 samples described in the text. The curves show the fit results.

then in a perfect detector the following decay rates would be observed :

$$f_{\pm}(\,\Delta t\,;\,\Gamma,\,\Delta m_d,\,\sin 2\beta) = \frac{1}{4}\,\Gamma\,\mathrm{e}^{-\Gamma|\Delta t|}\,[\,1\,\pm\,\sin 2\beta \times \sin \Delta m_d\,\Delta t\,] \tag{4}$$

where $\Delta t = t_{CP} - t_{tag}$ and the $(+)$ or $(-)$ sign indicates whether the B_{tag} is tagged as a B^0 or a $\overline{B}^0$ respectively. In the presense of the dilution factor $\mathcal{D}$ and Δt resolution $\mathcal{R}$ the observed rates become :

$$\mathcal{F}_{\pm}(\,\Delta t\,;\,\Gamma,\,\Delta m_d,\,\mathcal{D}\sin 2\beta,\,\hat{a}\,) = \frac{1}{4}\,\Gamma\,\mathrm{e}^{-\Gamma|\Delta t|}\,[\,1\,\pm\,\mathcal{D}\sin 2\beta \times \sin \Delta m_d\,\Delta t\,] \otimes \mathcal{R}(\,\Delta t\,;\,\hat{a}\,) \tag{5}$$

The time dependent decay rate asymmetry $\mathcal{A}_{CP}(\Delta t)$ is a CP–violating observable which (neglecting resolution effects) is approximately proportional to $\sin 2\beta$:

$$\mathcal{A}_{CP}(\Delta t) \;=\; \frac{\mathcal{F}_{+}(\Delta t)\;-\;\mathcal{F}_{-}(\Delta t)}{\mathcal{F}_{+}(\Delta t)\;+\;\mathcal{F}_{-}(\Delta t)} \;\sim\; \mathcal{D}\sin 2\beta \times \sin \Delta m_d\,\Delta t \tag{6}$$

7.1 Analysis procedure

The extraction of $\sin 2\beta$ from the data follows the following steps :

- Selection of the signal $B^0/\overline{B}^0 \to J/\psi\,K^0_S$ and $B^0/\overline{B}^0 \to \psi(2S)K^0_S$ events, detailed in the following section. Backgrounds and in particular any admixture with the "wrong" CP content have to be kept at a minimum level.

- Measurement of Δt. The resolution is studied using simulated events and its parameters are actually extracted from real data, as described in section 4.3.

- Determination of the flavor of the B_{tag}, as described in section 4.2. The dilution factors $\mathcal{D}_i$ for each tagging category are measured on real data, as described in section 6.

- Extraction of the amplitude of the *CP* asymmetry and the value of $\sin 2\beta$ with an unbinned maximum likelihood fit, desribed in the following.

A blind analysis has been adopted for the extraction of $\sin 2\beta$. A technique that hides the result of the fit by arbitrarily flipping its sign and adding an arbitrary offset, without affecting the error on the fitted parameters or their correlations, was used. Moreover, the visual *CP* asymmetry in the Δt distribution is hidden by multiplying Δt by the sign of the tag and adding an arbitrary offset. Such an approach allows to optimise and finalise the event selection and fitting strategy as well as perform a variety of validation and stability checks without the posibility of any experimenter's bias.

7.2 Event samples

The *CP* sample contains B^0 candidates reconstructed in the *CP* eigenstates $J/\psi K^0_S$ or $\psi(2S)K^0_S$. The charmonium mesons are reconstructed through their decays to e^+e^- and $\mu^+\mu^-$, while the $\psi(2S)$ is also reconstructed through its decay to $J/\psi\pi^+\pi^-$. The K^0_S is reconstructed through its decays to $\pi^+\pi^-$ and $\pi^0\pi^0$.

Utilisation of the exclusively reconstructed B samples (section 4.1) for the characterisation of the tagging and vertexing performance and quality has already been described. In addition 570 $B^+ \to J/\psi K^+$ candidates and 237 $B^0 \to J/\psi\,(K^{*0} \to K^+\pi^-)$ candidates have been reconstructed and used extensively in validation analyses.

7.3 Selection of events in the *CP* sample

Events are required to have at least four reconstructed charged tracks, a vertex within 0.5 cm of the average position of the interaction point in the transverse plane, total visible energy greater than 5 GeV, and second-order normalized Fox-Wolfram moment[4] ($R_2 = H_2/H_0$) less than 0.5.

For the J/ψ or $\psi(2S) \to e^+e^-$ ($\mu^+\mu^-$) candidates, at least one of the decay products is required to be positively identified as an electron (muon) in the EMC (IFR). Electrons outside the acceptance of the EMC are accepted if their DCH $\mathrm{d}E/\mathrm{d}x$ information is consistent with the electron hypothesis. Looser particle identification criteria are applied on the second electron (muon) candidates. In the muon case, a minimum ionising signature in the EMC is required.

J/ψ candidates are selected with an invariant mass greater than $2.95(3.06)\,\mathrm{GeV}/c^2$ for e^+e^- ($\mu^+\mu^-$) and smaller than $3.14\,\mathrm{GeV}/c^2$ in both cases. The $\psi(2S)$ candidates in leptonic modes must have a mass within $50\,\mathrm{MeV}/c^2$ of the $\psi(2S)$ mass. The lower bound is relaxed to $250\,\mathrm{MeV}/c^2$ for the e^+e^- mode. For the $\psi(2S) \to J/\psi\pi^+\pi^-$ mode, mass-constrained J/ψ candidates are combined with pairs of oppositely charged tracks considered as pions, and $\psi(2S)$ candidates with mass between $3.0\,\mathrm{GeV}/c^2$ and $4.1\,\mathrm{GeV}/c^2$ are retained. The mass difference between the $\psi(2S)$ candidate and the J/ψ candidate is required to be within $15\,\mathrm{MeV}/c^2$ of the known mass difference.

K^0_S candidates reconstructed in the $\pi^+\pi^-$ mode are required to have an invariant mass, computed at the vertex of the two tracks, between $486\,\mathrm{MeV}/c^2$ and $510\,\mathrm{MeV}/c^2$ for the $J/\psi K^0_S$ selection, and between $491\,\mathrm{MeV}/c^2$ and $505\,\mathrm{MeV}/c^2$ for the $\psi(2S)K^0_S$ selection.

For the $J/\psi K^0_S$ mode we also consider the decay of the K^0_S into $\pi^0\pi^0$. For pairs of π^0 candidates with total energy above 800 MeV we determine the most probable K^0_S decay point along the path defined by the K^0_S momentum vector and the primary vertex of the event. The decay-point probability is the product of the χ^2 probabilities for each photon pair constrained to the π^0 mass. We require the distance from the decay point to the primary vertex to be between -10 cm and $+40$ cm and the K^0_S mass measured at this point to be between 470 and $536\,\mathrm{MeV}/c^2$.

B_{CP} candidates are formed by combining mass-constrained J/ψ or $\psi(2S)$ candidates with mass-constrained K^0_S candidates. Cuts on the colinearity of flight vertex and momentum of the K^0_S (for $\pi^+\pi^-$ decays), the cosine of the helicity angle of the J/ψ or $\psi(2S)$ in the B candidate rest frame (e^+e^- and $\mu^+\mu^-$ modes) or the cosine of the angle between the B_{CP} candidate three-momentum vector and the thrust vector of the rest of the event ($\psi(2S) \to J/\psi\,\pi^+\pi^-$ mode) are applied to achieve the required signal purity.

B_{CP} candidates are identified in the $m_{\rm ES}$–ΔE plane (see section 4.1). Signal event yields and purities, determined from a fit to the $m_{\rm ES}$ distributions after selection on ΔE, are presented in Table 2. The *CP* candidate events are 168 with a purity of 95.6%. In 120 of these events there is information on the flavor of the other B. These events are used in the final fit for sin2β. Distributions of ΔE and $m_{\rm ES}$ are shown in Figures 5 and 6.

Final state	All events	Purity	Tagged events
$J/\psi\,K^0_S$ ($K^0_S \to \pi^+\pi^-$)	124	96%	85
$J/\psi\,K^0_S$ ($K^0_S \to \pi^0\pi^0$)	18	91%	12
$\psi(2S)K^0_S$	27	93%	23

Table 2: Event yields for the *CP* samples used in this analysis. The total number of events in the $m_{\rm ES}$–ΔE signal box and their purity, as well as the size of the subsamples where the other B is tagged, are shown.

7.4 Extracting sin2β

The Δt of the 120 selected and tagged events is fitted to the expected time evolution (equation 5) with an unbinned maximum likelihood fit. Individual event errors on Δt are taken into account. The resolution determined on the fully reconstructed sample and the mistag factor w_i corresponding to the tagging category for each event are used in the fit. The Δm_d are fixed to the nominal PDG [5] values of $\tau_{B^0} = 1.548$ ps and $\Delta m_d = 0.472\,\hbar\,\mathrm{ps}^{-1}$ respectively. The resulting errors on sin2β due to these uncertainties are 0.002 and 0.015.

7.5 Fit validation, systematics studies and null *CP* tests

Knowledge of the mistag fractions, description of the Δt resolution and backgrounds are (in that order) the main sources of systematic errors. All these have been extracted from real data. Real data, fully simulated Monte Carlo, and "Toy" Monte Carlo samples have been used to validate the method and implementation of the fit, to rule out possible biases from the method itself, and to assess the size of systematic errors.

The full CP analysis and fit were performed on data samples that have no *CP* asymmetry. No significant apparent *CP* effect was measured, as shown in Table 3. The 1.9 σ asymmetry in the $J/\psi\,K^{*0}$ channel is interpreted as a statistical fluctuation.

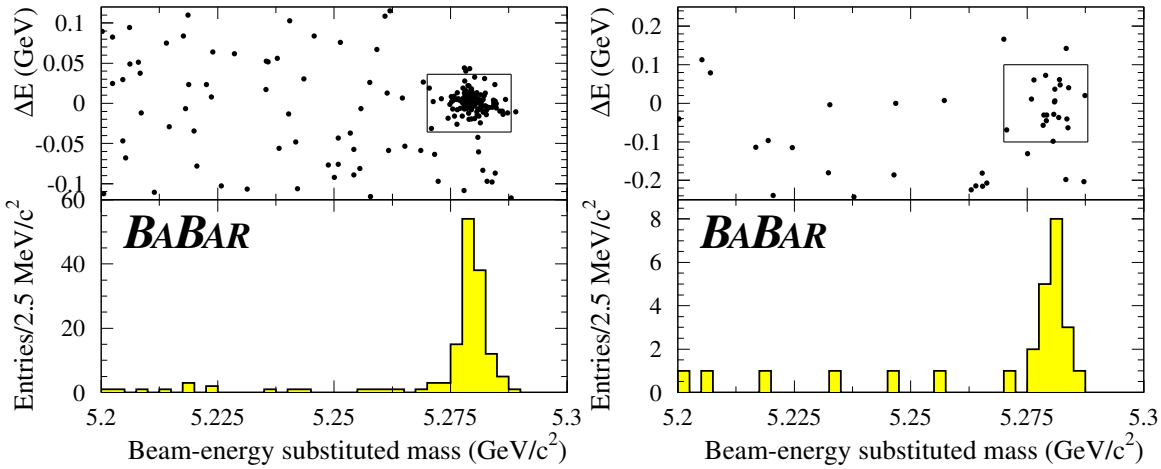

Figure 5: $J/\psi K_S^0$ signal. Left: $K_S^0 \to \pi^+\pi^-$, Right: $K_S^0 \to \pi^0\pi^0$

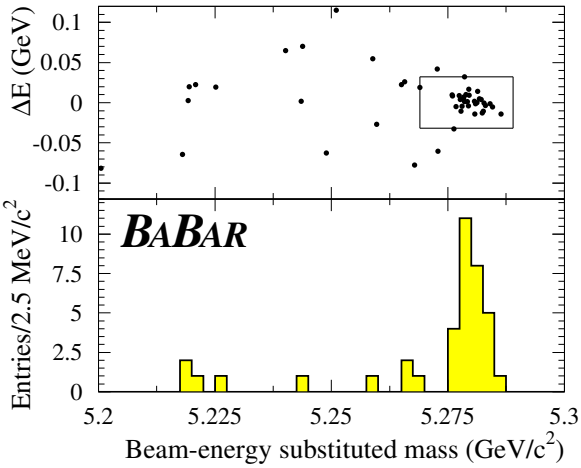

Figure 6: $\psi(2S)K_S^0$ ($K_S^0 \to \pi^+\pi^-$) signal.

Sample	Apparent CP-asymmetry
Hadronic charged B decays	0.03 ± 0.07
Hadronic neutral B decays	-0.01 ± 0.08
$J/\psi K^+$	0.13 ± 0.14
$J/\psi K^{*0}$ ($K^{*0} \to K^+\pi^-$)	0.49 ± 0.26

Table 3: Results of fitting for apparent CP asymmetries in various charged or neutral flavor-eigenstate B samples.

7.6 Results

The maximum-likelihood fit for sin2β on the full tagged sample of $B^0/\overline{B}^0 \to J/\psi K^0_S$ and $B^0/\overline{B}^0 \to \psi(2S)K^0_S$ events yields the preliminary result :

$$\sin 2\beta = 0.12 \pm 0.37\,(\text{stat}) \pm 0.09\,(\text{syst}) \tag{7}$$

The results of the fit for each type of *CP* sample and for each tagging category are given in Table 4. The contributions to the systematic uncertainty are summarized in Table 5. The Δt distributions for B^0 and $\overline{B}^0$ tags are shown in Fig. 7 and the raw asymmetry as a function of Δt is shown in Fig. 8. The probability of obtaining a value of the statistical error larger than the one we observe is estimated at 5%. Based on a large number of full Monte Carlo simulated experiments with the same number of events as our data sample, we estimate that the probability of finding a lower value of the likelihood than our observed value is 20%.

sample	sin2β
CP sample	**0.12±0.37**
$J/\psi K^0_S$ ($K^0_S \to \pi^+\pi^-$) events	-0.10 ± 0.42
other *CP* events	0.87 ± 0.81
`Lepton`	1.6 ± 1.0
`Kaon`	0.14 ± 0.47
`NT1`	-0.59 ± 0.87
`NT2`	-0.96 ± 1.30

Table 4: sin2β fit results from the entire *CP* sample and various subsamples.

Source of uncertainty	Uncertainty on sin2β
uncertainty on τ^0_B	0.002
uncertainty on Δm_d	0.015
uncertainty on Δz resolution for *CP* sample	0.019
uncertainty on time-resolution bias for *CP* sample	0.047
uncertainty on measurement of mistag fractions	0.053
different mistag fractions for *CP* and non-*CP* samples	0.050
different mistag fractions for B^0 and $\overline{B}^0$	0.005
background in *CP* sample	0.015
total systematic error	**0.091**

Table 5: Summary of systematic uncertainties on sin2β

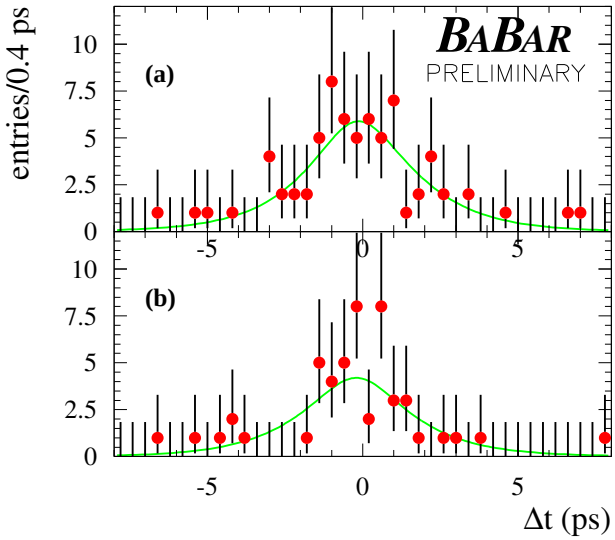

Figure 7: Distribution of Δt for (a) the B^0 tagged events and (b) the $\overline{B}^0$ tagged events in the *CP* sample. The error bars plotted for each data point assume Poisson statistics. The curves correspond to the result of the unbinned maximum-likelihood fit and are each normalized to the observed number of tagged B^0 or $\overline{B}^0$ events.

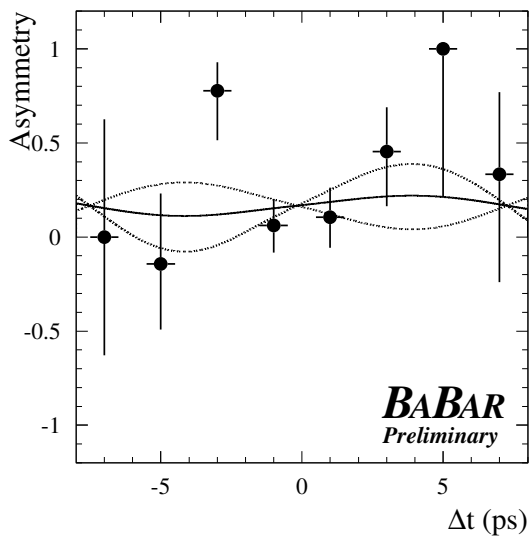

Figure 8: The raw B^0-$\overline{B}^0$ asymmetry $(N_{B^0} - N_{\overline{B}^0})/(N_{B^0} + N_{\overline{B}^0})$ with binomial errors as function of Δt. The solid curve represents our central value of $\sin 2\beta$. The two dotted curves correspond to one statistical standard deviation from the central value. The curves are not centered at $(0, 0)$ in part because the probability density functions are normalized separately for B^0 and $\overline{B}^0$ events, and our *CP* sample contains an unequal number of B^0 and $\overline{B}^0$ tagged events (70 B^0 versus 50 $\overline{B}^0$). The χ^2 between the binned asymmetry and the result of the maximum-likelihood fit is 9.2 for 7 degrees of freedom.

8 Conclusions and prospects

The first *BABAR* measurement of the *CP*-violating asymmetry parameter $\sin 2\beta$ has been presented :

$$\sin 2\beta = 0.12 \pm 0.37\,(\text{stat}) \pm 0.09\,(\text{syst}) \quad (preliminary) \tag{8}$$

BABAR aims at collecting more than 20 fb^{-1} of data by the end of Run 1 in fall 2000. A measurement of $\sin 2\beta$ with a precision better than 0.2 is expected early in 2001.

Very competitive preliminary results have also been presented for the B meson lifetimes, as well as the first measurements of $B^0\overline{B}^0$ mixing at the $\Upsilon(4S)$. These measurements will also benefit in the near future from the expected significant increase in statistics.

References

[1] C. Jarlskog, in *CP Violation*, C. Jarlskog ed., World Scientific, Singapore (1988).

[2] *BABAR* Collaboration, B. Aubert *et al.*, "The first year of the *BABAR* experiment at PEP-II", *BABAR*-CONF-00/17, submitted to the XXXth International Conference on High Energy Physics, Osaka, Japan.

[3] ARGUS collaboration, H. Albrecht *et al.*, Z Phys. **C48**, 543 (1990).

[4] G. C. Fox and S. Wolfram, Phys. Rev. Lett. **41**, 1581 (1978).

[5] Particle Data Group, D. E. Groom *et al.*, Eur. Phys. Jour. C **15**, 1 (2000).